SPECIAL FEATURE: DYNAMIC DESERTS

Constraints on shrub cover and shrub–shrub competition in a U.S. southwest desert

Wenjie Ji [ID],[1],† Niall P. Hanan,[1] Dawn M. Browning [ID],[2,3] H. Curtis Monger,[4] Debra P. C. Peters,[2,3] Brandon T. Bestelmeyer,[2,3] Steve R. Archer,[5] C. Wade Ross,[1] Brianna M. Lind,[1] Julius Anchang,[1] Sanath S. Kumar,[1] and Lara Prihodko[6]

[1]Plant and Environmental Sciences, New Mexico State University, Skeen Hall, Las Cruces, New Mexico 88003 USA
[2]USDA-ARS, Jornada Experimental Range, P.O. Box 30003, MSC 3JER, Las Cruces, New Mexico 88003 USA
[3]Jornada Basin Long Term Ecological Research Program, New Mexico State University, P.O. Box 30003, MSC 3JER, Las Cruces, New Mexico 88003 USA
[4]USDA-NRCS National Soil Survey Center, 100 Centennial Mall, Lincoln, Nebraska 68508 USA
[5]School of Natural Resources & the Environment, ENR2-N358, University of Arizona, Tucson, Arizona 85721 USA
[6]Animal and Range Science, New Mexico State University, Knox Hall, Las Cruces, New Mexico 88003 USA

Abstract. The cover of woody perennial plants (trees and shrubs) in arid ecosystems is at least partially constrained by water availability. However, the extent to which maximum canopy cover is limited by rainfall and the degree to which soil water holding capacity and topography impacts maximum shrub cover are not well understood. Similar to other deserts in the U.S. southwest, plant communities at the Jornada Basin Long-Term Ecological Research site in the northern Chihuahuan Desert have experienced a long-term state change from perennial grassland to shrubland dominated by woody plants. To better understand this transformation, and the environmental controls and constraints on shrub cover, we created a shrub cover map using high spatial resolution images and explored how maximum shrub cover varies with landform, water availability, and soil characteristics. Our results indicate that when clay content is below ~18%, the upper limit of shrub cover is positively correlated with plant available water as mediated by surface soil clay influence on water retention. At surface soil clay contents >18%, maximum shrub cover decreases, presumably because the amount of water percolating to depths preferentially used by deep-rooted shrubs is diminished. In addition, the relationship between shrub cover and density suggests that self-thinning occurs in denser stands in most landforms of the Jornada Basin, indicating that shrub–shrub competition interacts with soil properties to constrain maximum shrub cover in the northern Chihuahuan Desert.

Key words: Jornada Basin Long-Term Ecological Research (LTER); shrub–shrub competition; Southwestern U.S. drylands; Special Feature: Dynamic Deserts; woody plant encroachment.

Received 31 August 2018; revised 6 December 2018; accepted 21 December 2018. Corresponding Editor: Sujith Ravi.

† **E-mail:** wenjieji@nmsu.edu

INTRODUCTION

The proliferation and range expansion of woody plant species in arid and semi-arid ecosystems, also known as woody plant encroachment, has been observed worldwide by many researchers (Archer et al. 1988, Van Auken 2000, Asner et al. 2003, Eldridge et al. 2011). The

cover and dynamics of woody plants are, to a large extent, controlled by the availability of water in dryland ecosystems (Noy-Meir 1973). The upper limit of woody plant cover has been observed to be strongly related to precipitation in semi-arid tropical savannas (Sankaran et al. 2005, Good and Caylor 2011, Lehmann et al. 2014, Axelsson and Hanan 2017, 2018) and temperate semi-arid grasslands (Scholtz et al. 2018).

At landscape scales, topo-edaphic heterogeneity can have important local influences on woody plant distribution and density (McAuliffe 1994, Parker 1995, Monger and Bestelmeyer 2006). Vertical movement of water is largely controlled by soil texture and depth, with coarse-textured sandy soils allowing precipitation to penetrate into the soil, while shallow, crusted, and fine-textured soils tend to inhibit infiltration and percolation and promote lateral redistribution of water (runoff) during rainfall events (Buxbaum and Vanderbilt 2007, Ross et al. 2018). Thus, woody plants with deeper roots are more productive on sandy soils than clayey soils in the most arid climates while in less arid climates woody plant production may be greater on clayey soils (i.e., the inverse texture effect; Noy-Meir 1973). Topography also regulates the horizontal redistribution of water by creating spatial variability in runoff and run-on patterns, which sometimes overrides the effect of soil texture on the abundance of woody and herbaceous plant species (Wu and Archer 2005). Thus, spatial variations in soil properties and topography lead to differences in the transfer and storage of water across the landscape. As a result, vegetation patterns supported by such landscapes can be extremely complex, even with a spatially homogenous precipitation regime (Archer 1995, Bestelmeyer et al. 2006, Wheeler et al. 2007).

Variation in water availability can also lead to variations in vegetation structure (i.e., size and density). Maximum plant size is ultimately governed by the local availability of resources, such that shrub size in drylands tends to increase with water availability (Kempes et al. 2011), until reaching the point where their ability to maintain continuity in xylem water transport on a given soil texture, depth, or topographic location is jeopardized and leads to branch mortality (Sperry and Hacke 2002, Hacke et al. 2006). At stand level, water uptake by a population of

shrubs can be approximated as proportional to the product of mean plant size and plant density (Sea and Hanan 2012). With increasing shrub size and density, water may become limiting and self-thinning occurs where shrub size and density are related to each other via characteristic log-log relationships that are diagnostic of intra-specific (in our case shrub–shrub) competition (Weller 1987, Enquist et al. 1998, Sea and Hanan 2012).

The Jornada Basin Long-Term Ecological Research (LTER) site sits at the northern edge of the Chihuahuan Desert and, similar to other deserts in the U.S. southwest, plant communities have experienced a major shift from perennial grasslands to woody plant dominated shrublands over the past 150 yr (Buffington and Herbel 1965, Gibbens et al. 2005). The spatial pattern of these state changes is known to be influenced by variations in historical grazing pressure, contagious shrub spread, and shrub removal (Peters et al. 2006, Bestelmeyer et al. 2011, 2018). Although there have been several recent efforts to understand patterns of shrub encroachment at relatively fine scales (e.g., Goslee et al. 2003, Laliberte et al. 2004, Browning et al. 2012), it is still unclear why remnant grass patches have persisted in certain areas while other areas have become dominated by shrubs.

In an effort to better understand broad-scale vegetation dynamics in relation to topo-edaphic heterogeneity, we created a high spatial resolution (1 m) shrub map of the Jornada Basin LTER using multi-spectral (4-band) aerial photography. We then explored some of the possible determinants of shrub cover. Similar to Sankaran et al. (2005), we hypothesized that the potential upper limit of shrub cover in the Jornada Basin would be determined mainly by water availability. However, since long-term average precipitation is similar across the Jornada Basin floor, we hypothesized that water availability controlled by soil texture and topography would be the dominant control of spatial variation in woody plant cover and structure (i.e., size and density). More specifically, following predictions of the inverse texture effect in arid climates (Noy-Meir 1973, Ward et al. 2013), we expected that the upper limit of shrub cover would be higher on coarse-textured sandy soils relative to fine-textured clayey soils, and higher in topographic settings receiving run-on from upslope than in

locations losing incoming precipitation in runoff. In addition to analyzing patterns in maximum canopy cover, we also examined patterns in shrub size and density (self-thinning) as a diagnostic of density dependence and shrub–shrub competition constraints on maximum shrub cover.

METHODS

Study area

The Jornada Basin LTER site includes both the U.S. Department of Agriculture-Agricultural Research Service (USDA-ARS) Jornada Experimental Range (JER, 78,413 ha) and the New Mexico State University-owned Chihuahuan Desert Rangeland Research Center (CDRRC, 24,960 ha; Fig. 1). The elevation range of the study area is 1214–1768 m a.s.l. (excluding the mountain areas).

The climate of the Jornada is characterized by hot summers with monsoon rainfall, and cool, dry winters. Mean maximum monthly air temperature ranges from 13.7°C in January to 34.9°C in July (96-yr average from 1915 to 2010, using data retrieved on 31 May 2018 from https://jornada.nmsu.edu/content/jer-standard-gauge-monthly-precipitation-data). Long-term mean annual precipitation ranges from 203 mm on basin floors to 250 mm on piedmont slopes, 64% of which is received in summer (July–October; long-term precipitation data from 1915 to 2000, data retrieved on 31 May 2018 from https://jornada.nmsu.edu/content/usda-noaa-nws-daily-climatological-data). Summer precipitation originates in the Gulf of Mexico and California and often
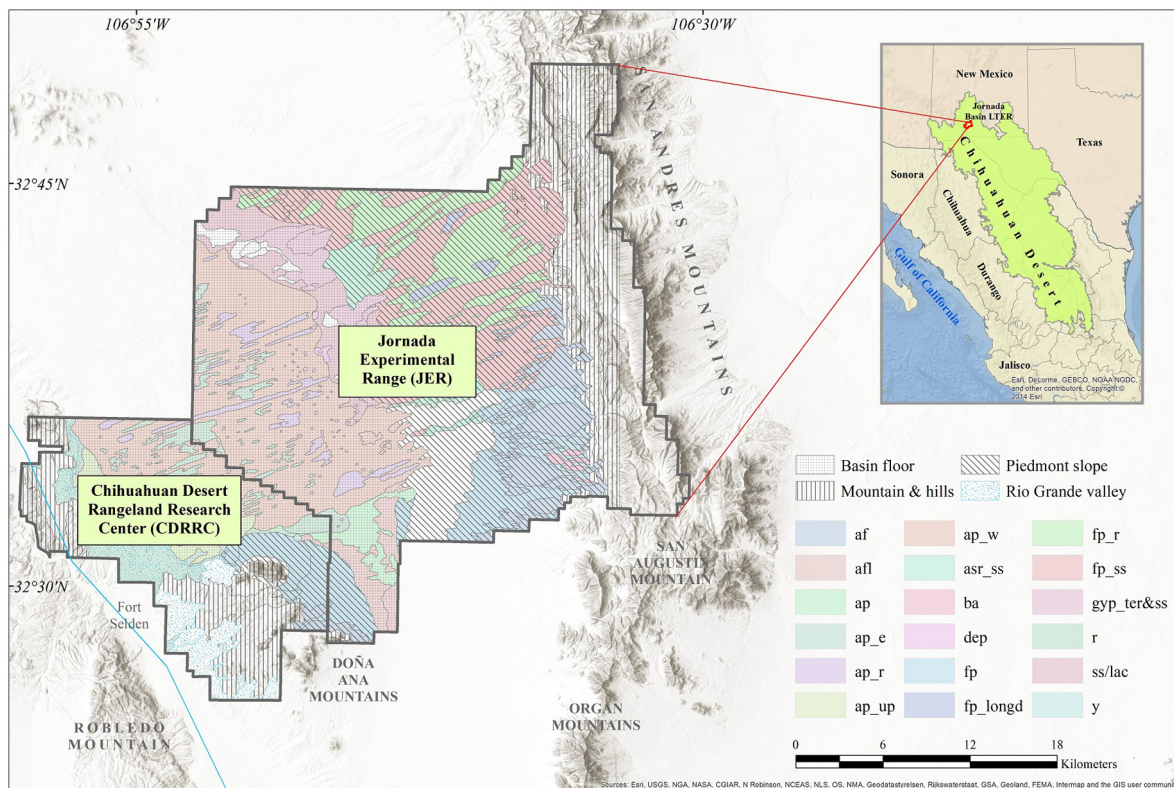

Fig. 1. The 103,373 ha Jornada Basin Long-Term Ecological Research site in the northern Chihuahuan Desert (inset) includes both the U.S. Department of Agriculture-Agricultural Research Service Jornada Experimental Range (JER) and the New Mexico State University Chihuahuan Desert Rangeland Research Center (CDRRC). Names corresponding the landform codes in legend are given in Table 1. Detailed descriptions of the landforms can be found in Monger et al. (2006).

occurs as intense convective storms that are highly localized, while winter precipitation is of lower intensity and arises from broad frontal storms originating over the Pacific Ocean.

Plant communities over the past 150 yr at the Jornada Basin LTER site have transformed from grasslands dominated by *Bouteloua eriopoda* (black grama) in uplands and *Pleuraphis mutica* (tobosa) in playas to shrublands that are spatially segregated by topographic position and soil texture: *Prosopis glandulosa* (honey mesquite) predominates on sandy plains, *Larrea tridentata* (creosote bush) on gravelly upper piedmont soils, and *Flourensia cernua* (tarbush) on finely textured lower piedmont and basin floor soils. Other common plant species include: *Scleropogon brevifolius* (burrograss), *Sporobolus* spp. (dropseeds), *Muhlenbergia porteri* (bush muhly), *Gutierrezia sarothrae* (snakeweed), *Atriplex canescens* (four-wing saltbush), *Ephedra* spp. (Mormon tea), and *Yucca* spp. (soaptree yucca; species list was obtained from https://jornada.nmsu.edu).

Shrub cover, patch size, and patch density from aerial photographs

We used National Agriculture Imagery Program (NAIP) imagery acquired on 21 May 2011 to generate a shrub cover map of the Jornada Basin LTER. Given that year-to-year change in woody cover is generally small (Axelsson and Hanan 2018), 2011 estimates are considered to reasonably represent shrub cover across the Jornada during the recent 10–15 yr. National Agriculture Imagery Program images have a 1-m spatial resolution and four spectral bands (red, green, blue, and near-infrared). The May 2011 image date coincides with peak shrub canopy greenness which occurs before peak grass greenness in summer months (Browning et al. 2018), maximizing our capacity to identify shrub cover. An unsupervised approach (Iterative Self-Organizing Data Analysis Technique) was used for image classification. To better distinguish woody plants from herbaceous cover and the soil background, texture features were used in addition to the NAIP spectral bands, as recommended by Basu et al. (2015). Thirty classes were initially produced by the unsupervised classification; these were then manually assigned as shrub or non-shrub. Necessary corrections of the classification (through combining and/or splitting of the

original thirty classes) were done manually while referencing co-located Google Earth imagery. Shrub cover was estimated at a 1-ha scale (100 × 100 m) by dividing the number of pixels classified as shrub by the total number (10,000) of 1 m^2 pixels within each 1-ha area. Shrub classification was particularly difficult in some parts of the southern JER (areas characterized by erosional scarplets and arcuate sand ridges; Monger et al. 2006) due to high local-scale variability of the patterns of vegetation and soil. These areas were therefore not included in this study (~11% of the Jornada Basin).

Accuracy of the shrub map was assessed using 200 random sample points. Ground truth of each random point (shrub or non-shrub) was determined using Google Earth imagery and then compared to the NAIP classification. Data collected on two independent projects were also used for accuracy assessment. As part of the 2011 Jornada Experiment campaign (JORNEX, Rango et al. 1998), vegetation measurements were taken at 10-cm intervals within 0–30 m, 60–90 m, and 120–150 m segments of each of five 150-m transects. Shrub cover was then summarized for every 10 m of the sampled segments, resulting in a total of 45 samples (*n* = 9 samples/transect × 5 transects). Shrub cover from image classification was estimated within a 5-m buffer area along each of these transect segments and then compared to field-estimated data. Shrub cover was also obtained from the PHENOMET project (Browning et al. 2017), which recorded vegetation cover (line-point intercept method) along five 50-m transects at three Jornada Basin LTER sites (GIBPE, SCAN, and TROMBLE; Herrick et al. 2005). Image-estimated shrub cover was summarized within a minimum bounding rectangle at each of the three sites and compared to the PHENOMET field data. Out of the 200 randomly sampled points on Google Earth, 184 were correctly classified (92%). Shrub cover estimated from image classification also showed a satisfactory agreement with ground-measured shrub cover from the independent field campaigns. The intercept and slope of a Model II regression line between the ground-measured and image-estimated shrub cover are 0.01 and 0.95, respectively (Fig. 2).

The raster shrub map was converted into polygons using ArcGIS tools (ESRI 2016). Due to the
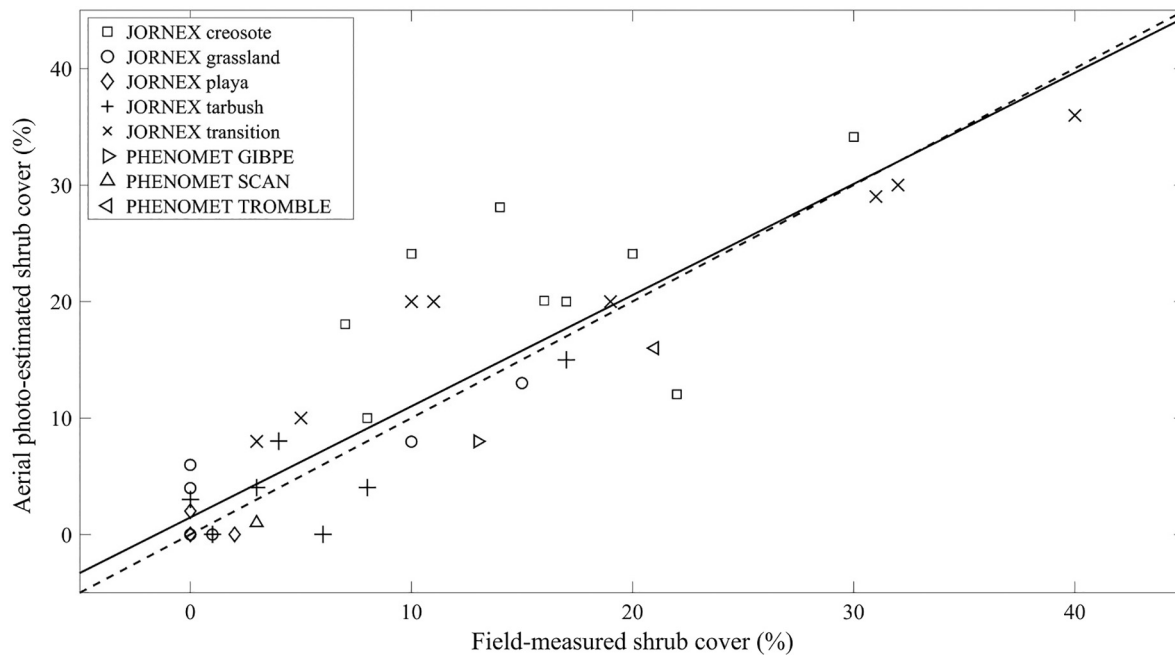
Fig. 2. Field-measured shrub cover (%) and aerial photo-estimated shrub cover (%) in the Jornada Basin. Field-measured shrub cover data are from the Jornada Experiment (JORNEX) and PHENOMET projects. Solid line is the Model II regression line. Dotted line represents the 1:1 line.

overlapping and clumping of the shrub canopies, we define each polygon as a shrub patch rather than an individual plant. Patch density (ha^{-1}) and mean patch size (m^2) were also estimated at hectare spatial resolution.

Landform, soil texture, and topography

We used a landform map developed from existing soil survey maps, stereo aerial photographs, Landsat satellite images, and digital elevation models (DEMs; Monger et al. 2006). The landform map depicts the Jornada Basin as having four major geomorphic components: mountains and hills, piedmont slopes (bajadas), basin floors, and Rio Grande Valley (Fig. 1). These components were further subdivided into 26 landform units. Detailed descriptions of the landform units are given in Monger et al. (2006). For this study, we ranked the landforms according to plant available water (PAW) based on our expert knowledge of soil texture, geomorphology, and topography (e.g., Monger et al. 2006, 2015; Table 1).

Soil texture data (percent clay, silt, and sand) were obtained from the global SoilGrids map

Table 1. Landforms ranked by plant available water (from low [rank 1] to high [rank 14]).

Rank	Landform name	Map code
1	Ballena	ba
2	Ridges and interridge valleys	r
3	Alluvial fan remnants	af
4	Gypsiferous terraces/sand sheets	gyp_ter & ss
5	Reddish brown sand sheets/dunes	fp_r
6	Longitudinal dunes	fp_longd
7	Alluvial plain†	ap
8	Sand sheets over gypsum	ss/lac
9	Sand sheets/coppice dunes	fp_ss
10	Arcuate sand ridges/sand sheets	asr_ss
11	Fan piedmont	fp
12	Alluvial flat	afl
13	Depressions	dep
14	Playas	y

Note: Detailed descriptions of the landforms can be found in Monger et al. (2006).
† Includes alluvial plain eroded (ap_e), alluvial plain sand sheets (ap_r), alluvial plain wind worked (ap_w), and alluvial plain uplifted (ap_up) in Monger et al. (2006).

(Hengl et al. 2017, data retrieved on 31 January 2018 from www.SoilGrids.org) at seven depths (0, 5, 15, 30, 60, 100, and 200 cm). To characterize infiltration, we calculated surface soil clay

content by averaging percentage clay of the first two depths (0 and 5 cm) using trapezoidal integration. The SoilGrids map has a spatial resolution of 250 m and was resampled (using nearest neighbor) to the same resolution as the shrub cover map (100 m). Saturated hydraulic conductivity (K_{sat}) was also estimated based on the lookup table provided by Clapp and Hornberger (1978).

We used the topographic wetness index (TWI, also known as the compound topographic index) as an indicator of the effect of topography on soil moisture. Topographic wetness index is calculated using the equation: TWI = ln (a/tan b), where a is the upstream contributing area (m^2) and b is the slope in radians (Beven and Kirkby 1979). Both the contributing area and slope were calculated from a DEM using ESRI ArcGIS tools (Flow Accumulation for contributing area and Slope for slope). Digital elevation model data were obtained from the U.S. Geological Survey (USGS) National Elevation Dataset (https://nationalmap.gov/elevation.html) with a spatial resolution of 1/3 arc-seconds (~10 m). High TWI values indicate topographic low points and drainage depressions (more run-on), whereas low TWI values are associated with crests and ridges (more runoff). A limitation in the calculation of TWI is that the Flow Direction tool in ArcGIS allows flow to pass to only one neighboring cell, which has been shown to be less accurate than considering multiple neighboring cells downslope (Rampi et al. 2014). For this application, however, we anticipated that TWI would provide a useful index of topographic controls on precipitation redistribution in the Jornada Basin landscape.

Statistical analysis

Since the maximum potential cover supported by a system should be reached only rarely, we consider the 99th percentile of shrub cover (either across the entire basin or on a given landform) as the upper limit in our analysis at the Jornada Basin.

We used Kendall's tau (τ; Helsel and Hirsch 2002) to test our hypothesis of the control of water availability on potential shrub cover. Correlation was calculated between the 99th percentile shrub cover and PAW ranks of each landform. A rejection of the null hypothesis (H_1)

would indicate a monotonic positive ($\tau > 0$) or negative ($\tau < 0$) relationship between water availability and potential shrub cover.

To explore the relationship between the potential upper limit of shrub cover (the 99th percentile) and soil texture (surface clay content) and topography (TWI), we used an additive nonparametric quantile regression analysis (Koenker et al. 1994) as implemented in the quantreg library (function rqss) of the statistical software package R (http://www.r-project.org/).

Linear quantile regression (function rq of the quantreg library in R) was used to explore the relationship between shrub patch size and patch density. We chose quantile regression instead of ordinary linear regression to reduce the impacts of disturbances (such as drought and herbivory) on shrub structure. We used the 95th percentile in our regression analysis so that a sufficient sample size (above the regression line) would be retained to draw statistical conclusions. Both size and density were ln-transformed prior to regression analysis.

Results

Spatial variation of shrub cover at the Jornada Basin LTER

Shrub cover at 1 ha scale varied considerably across the basin (Fig. 3). Mean shrub cover ranged from 3% to 27% across the landforms defined in Table 1, with 99th percentile shrub cover varying 28–69% (Fig. 4). The mean and 99th percentile shrub cover across the entire basin (i.e., all landforms combined) were 17% and 40%, respectively. Mean shrub cover in JER (Fig. 1) was highest on sand sheets to the northeast of the basin (reddish brown sand sheets and dunes, sand sheets and coppice dunes) and in depressions and depression margins not subject to regular or long-duration inundation. The highest mean shrub cover in CDRRC was observed on uplifted (20%) and wind worked (18%) alluvial plains. Kendall's τ test showed significant increases in the upper limits of shrub cover (99th percentile) with increasing PAW, as indexed by our expert ranking of the different landforms ($P = 0.02$, excluding playas that are ephemerally flooded, with little or no shrub cover). The relationship between potential shrub cover and water availability was further strengthened when
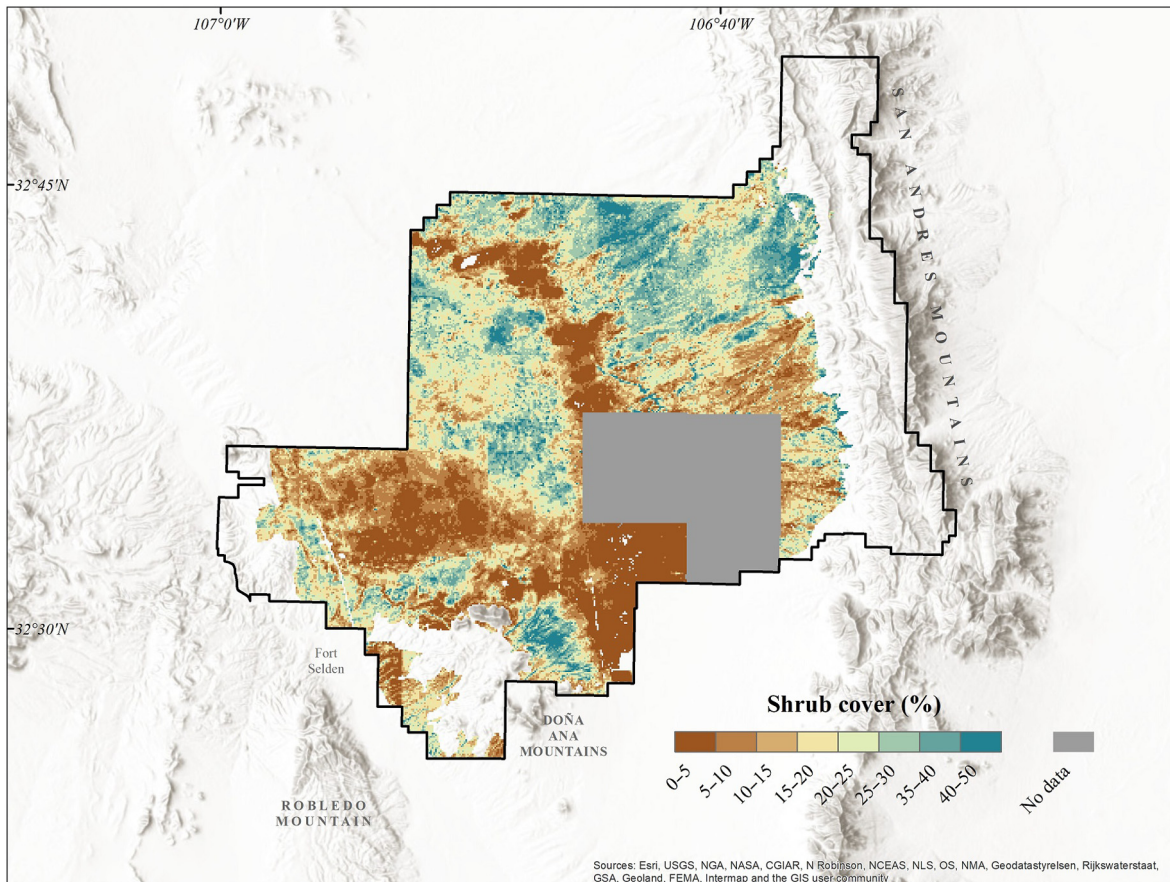
Fig. 3. Shrub cover (%) in the 103,373 ha Jornada Basin Long-Term Ecological Research site in 2011 derived from airborne 1 m resolution imagery and aggregated at 1 ha scale. Solid gray shading indicates missing data in a part of the basin with particularly high local-scale variability where shrub cover has not yet been estimated, while un-shaded areas on the E, W, and SW margins of the Jornada Experimental Range and Chihuahuan Desert Rangeland Research Center are mountainous and/or rocky regions not included in this study. Note vertical and horizontal linear features in the central region of this map correspond to fence-lines with differing management history.

gypsiferous sand sheets (where vegetation is limited by high gypsum content), alluvial flats (which have high herbaceous cover due to run off from the piedmont slope), and playa (which is ephemerally flooded and has little or no shrub cover) were excluded from the analyses ($P < 0.01$).

Shrub cover variations relative to soil clay content and TWI

Surface clay content ranged from 11% to 42% across the Jornada Basin. Soils on sand sheets and sand dunes are generally coarser, while higher clay content increases in landforms that

receive more run-on water (e.g., depressions and playas). Results of the quantile regression analysis showed that maximum potential shrub cover initially increased with surface clay content, then decreased as clay content surpassed 18% (Fig. 5). K_{sat} estimates suggest that water infiltration declines rapidly as clay content increases above 19%, close to the inflection point observed in maximum shrub canopy cover (18%). We acknowledge that K_{sat} estimates using a model based on texture (in this case Clapp and Hornberger 1978) are highly uncertain and impacted by local differences in soil characteristics, vegetation, and biota (Whitford 1996, Rango et al.
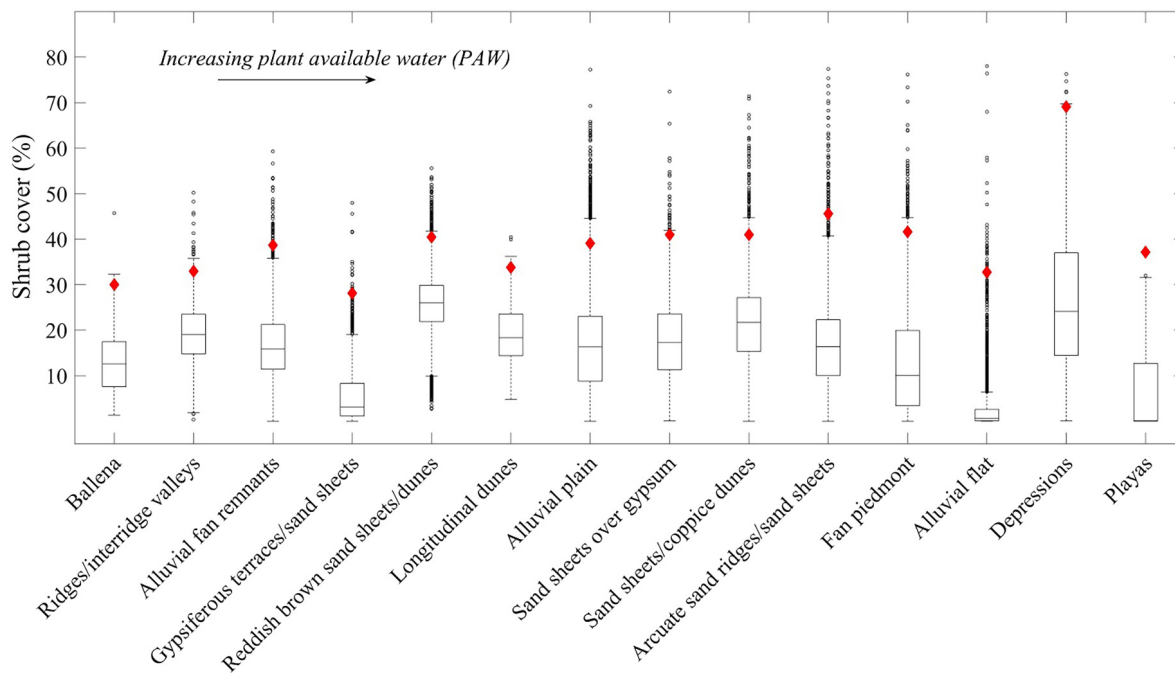
Fig. 4. Shrub cover (%) by landform types. The center, bottom, and top of boxes indicate the median, the 25th percentile, and the 75th percentile, respectively. Red diamonds are the 99th percentiles of shrub cover.

2003). However, this close correspondence strongly suggests that reduced infiltration may drive the change in observed maximum cover at increasing clay content.

The TWI provides an alternative perspective on water availability based primarily on landscape position and potential for redistribution of water. However, while TWI values varied markedly across the Basin, reflecting the topographic heterogeneity and complexity of the Jornada Basin, no consistent or significant relationships were detected between the upper limit of shrub cover and TWI, either within landforms or across the entire basin (Fig. 6; quantile regression analysis, $P > 0.1$).

Shrub patch size and density

With the exception of gypsiferous terraces and sand sheets, alluvial flats, and playas, 95th quantile shrub patch size decreased with patch density (Fig. 7), as predicted for plant populations that are competing for resources and undergoing self-thinning. The slopes of the 95th percentile patch size–density regression lines on these sites ranged from −1.05 on ballenas to −1.45 on depressions (Appendix S1: Fig. S1, Table S1). In

locations above the 95th percentile regression line (i.e., the self-thinning lines), ballena landscapes had the smallest mean patch size (8.8 m^2) and highest mean patch density (335 ha^{-1}), while reddish brown sand sheets and dunes had the largest patch size (36.1 m^2) and lowest density (106 ha^{-1}) (Fig. 8).

Discussion

The 99th percentile shrub cover for the entire Jornada Basin is 40%, but the inferred maximum varies considerably from 28% to 69% among landforms within the basin (Fig. 4). In arid and semi-arid ecosystems, this upper limit in shrub cover is, at least in part, controlled by the amount of precipitation a region receives (Noy-Meir 1973, Fig. 9). However, the average value of 40% for the temperate Jornada Basin (MAP = 248 mm/yr) is nearly twice that predicted for tropical savannas at similar MAP (21% according to the relationship reported by Sankaran et al. 2005). This may reflect that, in temperate systems with lower annual potential evapotranspiration, a specified annual rainfall may support higher maximum cover of woody plants than similar
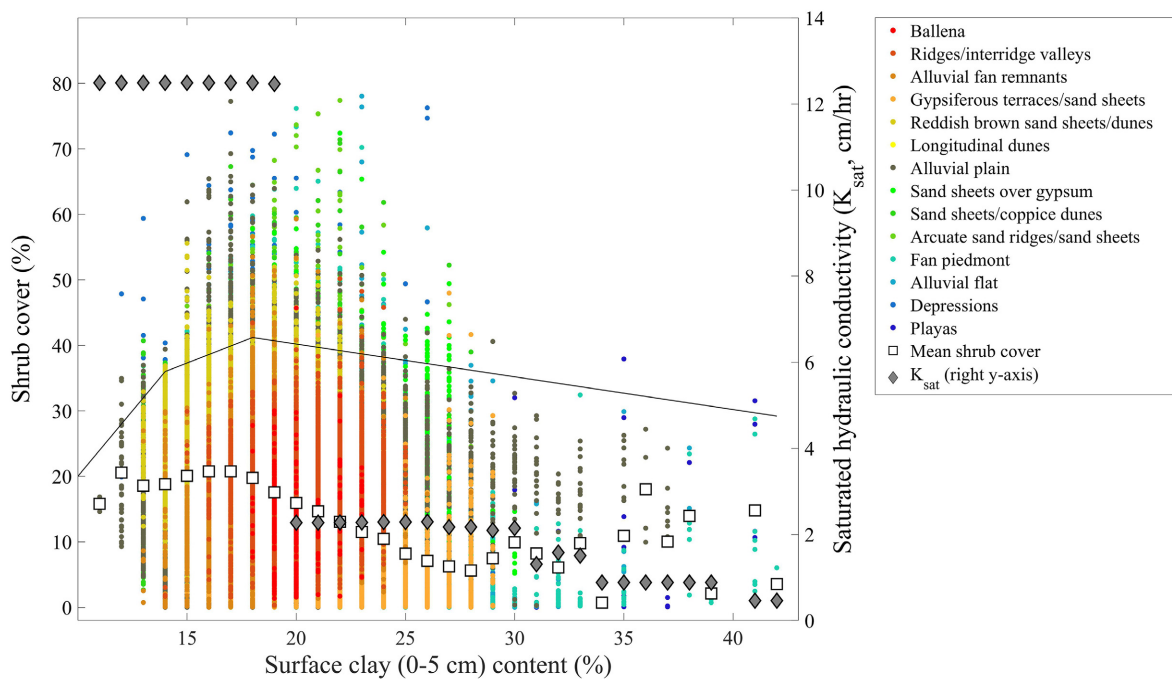
Fig. 5. Shrub cover (%) and surface (0–5 cm) clay content (%). Data points are color-coded by landform types. Solid line is the 99% quantile regression line. Open squares and filled diamonds are mean shrub cover and estimated saturated hydraulic conductivity (K_{sat}, cm/h), respectively. Note that not all data points are visible due to overlaps.

rainfall in a tropical system. The 40% maximum cover was also slightly higher when compared to the Santa Rita Experimental Range (SRER) in the Sonoran Desert (MAP = 370 mm/yr), where Browning et al. (2008) observed a maximum potential cover of ~30–35% using classified aerial photography. The lower maximum cover found at SRER may be related to a narrower focus on a single soil/landform type with a single woody species (*Prosopis velutina*) since a more synoptic assessment of shrub cover at the SRER using satellite remote sensing (Huang et al. 2007, 2018) suggests the Browning et al. (2008) estimate may be conservative at broader spatial scales.

Within the Jornada Basin, PAW at a given location reflects water redistribution, soil properties, and geomorphic characteristics (Duniway et al. 2018). Spatial variation in soil texture will dictate, to some extent, the spatial variation in potential shrub cover, as soil texture variations impose trade-offs in precipitation infiltration/percolation (hence the amount of water that might be preferentially available to deep-rooted shrubs) and soil fertility. Relative to clayey soils, sandy soils have

higher infiltration/percolation capacities but are more nutrient poor (Chapin et al. 2011). These trade-offs were evident in the patterns of maximum shrub cover potential we observed on Jornada Basin landforms (Fig 5). As the surface (0–5 cm) clay content increased from 11% to 18%, potential shrub cover increased from 20% to 40%, but as clay content rose above 18%, potential shrub cover steadily declined. The former represents the benefits of increasing fertility with increasing clay content with little downside for rainfall infiltration/percolation (water infiltration rate, as indicated by K_{sat}, was ~80 cm/h for soils with 11–19% clay). The latter, however, suggests that the benefits of increased fertility for shrubs are offset and constrained by reductions in rainfall infiltration/percolation (K_{sat} < 15 cm/h; at >20% clay). This is consistent with previous studies documenting that soils with high clay content were less prone to shrub encroachment in the U.S. southwest region (Browning et al. 2008, Rachal et al. 2012).

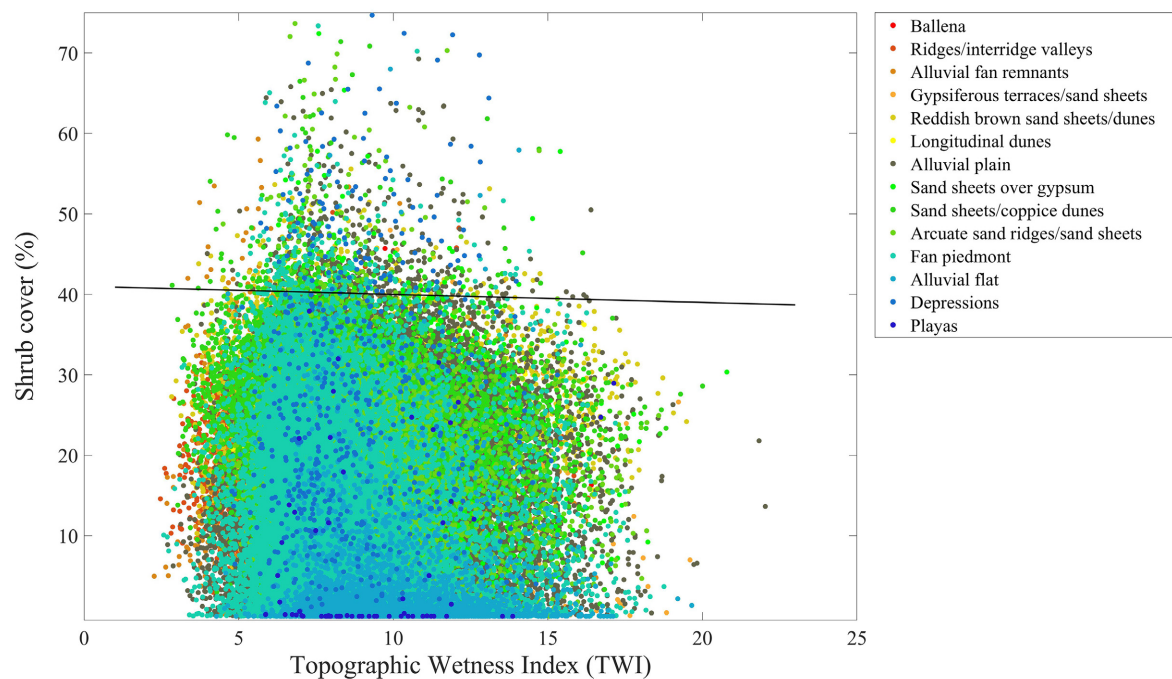The TWI failed to show any correlation with potential shrub cover (Fig. 6). One limitation of

Fig. 6. Relationship between shrub cover (%) and Topographic Wetness Index (TWI) values. Data points are color-coded by landform types. Solid line is the 99% quantile regression line. Note that not all data points are visible due to overlaps.

the TWI algorithm (see *Methods*) is that it considers only topography in directing water redistribution, with no specific consideration of infiltration/percolation rates or upslope soil properties and vegetation cover. Regarding the latter, TWI therefore ignores the feedback relationships between a given landscape setting and surrounding soils and vegetation, particularly the interactions between soils and vegetation patch spatial distributions on water redistribution (Ludwig et al. 2005). Thus, landscape connectivity indices that explicitly consider vegetation in their formulation (Ludwig et al. 2002, McGlynn and Okin 2006) may better characterize the complex patterns of redistribution of water (and other resources such as nutrients) between and within landscapes. Difficulties in separating bare ground from herbaceous cover limited our ability to calculate these more advanced metrics of connectivity and water redistribution.

Distinct self-thinning of the shrub patches was apparent in 11 of the 14 landforms in our basin-scale assessment (Fig. 7, Appendix S1: Fig. S1), which strongly indicates the presence of

competition among shrubs. However, this shrub–shrub competition is probably only active in locations where shrub cover is close to the maximum potential supported by a given landform. At early stages of shrub growth, or in settings where shrub cover is kept below the climatic/landform maxima by disturbance events (e.g., herbivory), shrub–shrub competition would presumably be muted. In locations where the history of climatic, biotic, and anthropogenic conditions has favored shrub establishment and survival, shrub cover may approach the maximum, either through growth in patch size or density. In these cases, further recruitment and growth may be increasingly inhibited due to stand-scale competition. This is consistent with observations that rates of shrub proliferation decrease with increases in shrub cover (e.g., Roques et al. 2001, Fensham et al. 2005, Axelsson and Hanan 2018) and reinforces that shrub–shrub competition, although not always active for shrubs at low density, is an important factor structuring shrub communities at the Jornada, in addition to the woody–herbaceous interactions
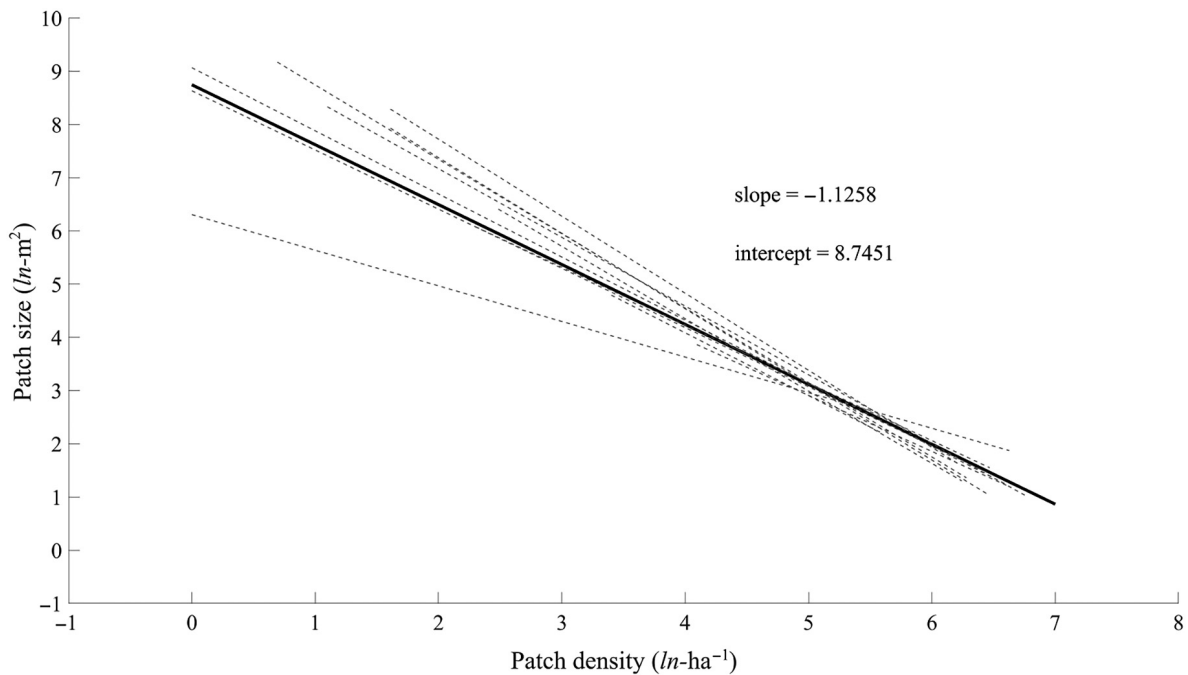
Fig 7. The 95th percentile regression lines between shrub patch size (ln-m^2) and patch density (ln-ha^{-1}) for 11 landforms (out of 14 total) across the Jornada Basin where distinct thinning lines were present (see Appendix S1: Fig. S1). Both size and density are ln-transformed. Solid line is all landforms combined and the dotted lines are individual landforms.

that are more typically invoked in arid ecosystems (Scholes and Archer 1997, Sankaran et al. 2004).

Resource availability limits maximum plant size (Ryan and Yoder 1997, Choi et al. 2016). Our results suggest that, in locations above the self-thinning lines on different landforms (Appendix S1: Fig. S1), mean shrub patch size was smaller on drier landforms and increased with PAW (Fig. 8; marginally significant according to Kendall's τ test, $P = 0.11$). When the trend for increasing patch size with PAW is combined with the observation that stand-level canopy cover is not generally correlated with patch density (Appendix S1: Fig. S2), but is highly correlated with mean patch size (Appendix S1: Fig. S3), we infer that the general trend to increasing shrub cover with PAW (Fig. 4) is driven primarily by increases in mean patch size, rather than increases in patch density. This is consistent with a recent study (Axelsson and Hanan 2017) that found increases in woody cover across an African savanna rainfall gradient were more closely related to crown size than density of shrubs and trees.

Shrubs have been proliferating in grasslands of the Jornada Basin over the past 150 yr, so shrub communities in most invaded grassland sites have had ample time to develop and mature. Although shrub cover maxima at the Jornada Basin appears to be constrained by water availability (as governed by landform and soil type), actual cover in many locations is considerably below the inferred upper limit (Fig. 9). In contrast to patterns observed in tropical savannas, where fire and herbivory are the main drivers of tree cover variability below the maximum (Sankaran et al. 2005, Archibald and Hempson 2016), it is less well known which factors maintain shrub cover at most locations in Jornada landscapes below their inferred potential. Data on local heterogeneity in historical establishment and mortality events related to clay mineralogy (e.g., soil shrink–swell capacity), drought (Reynolds et al. 1999, Peters et al. 2010), cattle grazing (Herbel et al. 1972, Gibbens et al. 2005), soil erosion
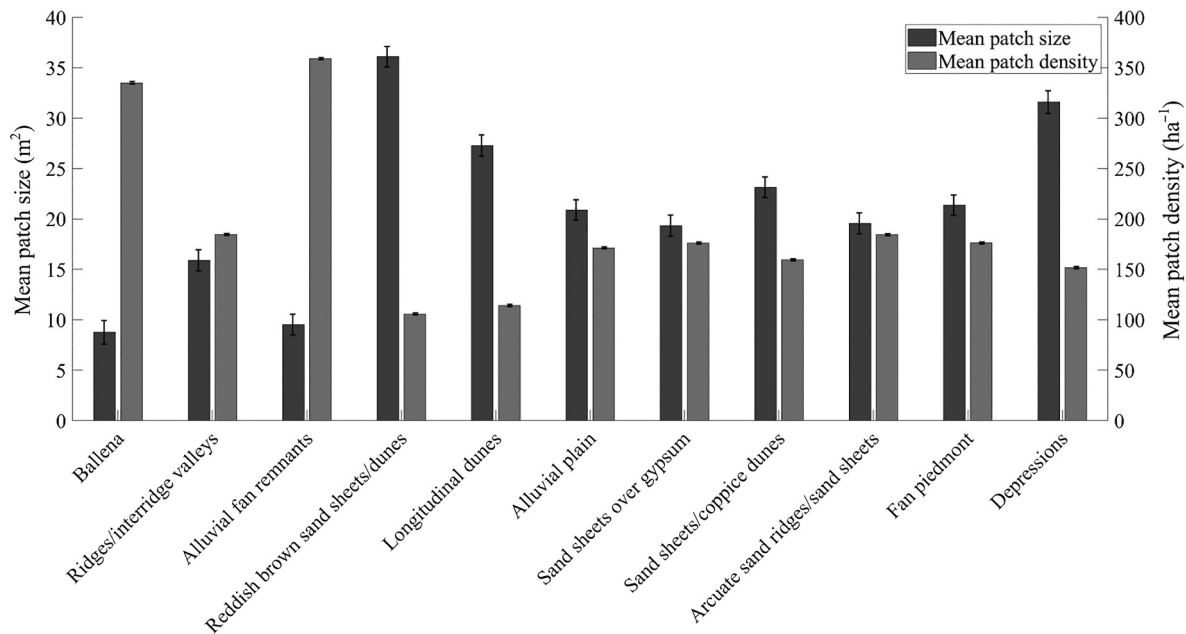
Fig. 8. Mean shrub patch size (m^2) and patch density (ha^{-1}) with standard error bars in locations above the 95th percentile regression line (i.e., in denser situations, where density-dependent competition and thinning are evident; Appendix S1: Fig. S1) on 11 landforms (out of 14 total) at the Jornada Basin.
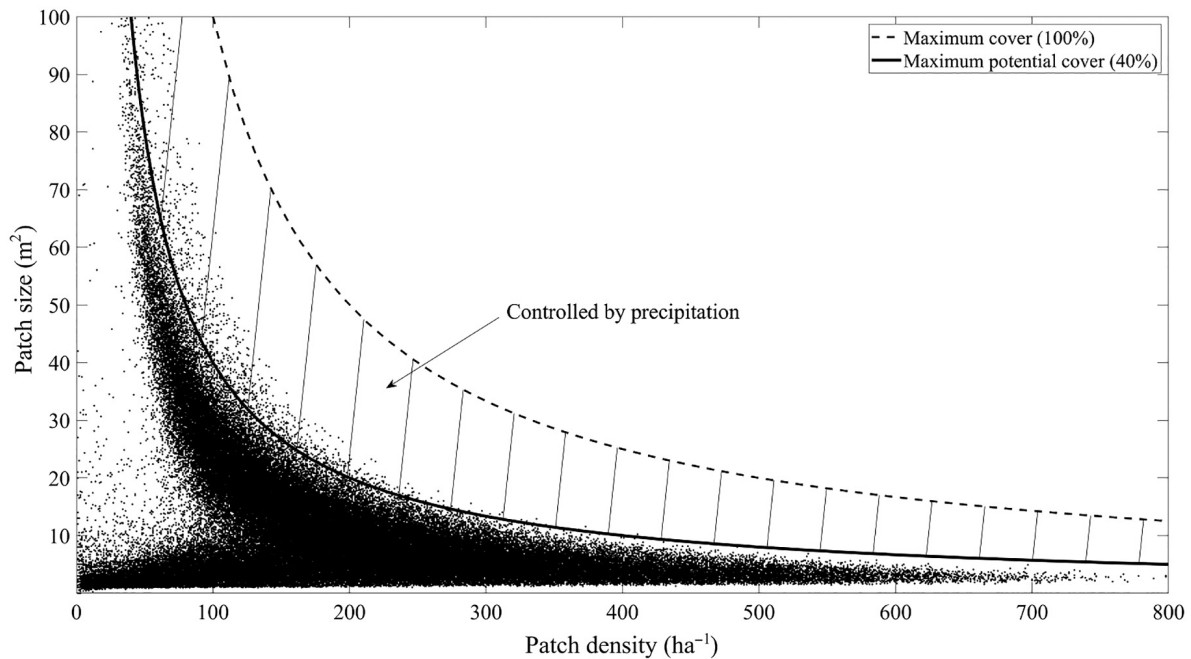

Fig. 9. Shrub patch size (m^2) and patch density (ha^{-1}) for all landforms within the Jornada Basin. The dotted line is the 100% cover line, and the solid line is the 40% cover line, where cover = patch density × patch size.

(Ludwig et al. 2005), and small mammal and insect herbivory and granivory (Whitford and Bestelmeyer 2006, Schooley et al. 2018) may be needed to explain what is preventing potential shrub cover from being realized at the Jornada Basin.

CONCLUSIONS

Water is a primary factor limiting vegetation composition and abundance in arid ecosystems. Our results suggest that, at the scale of the 103,373 ha Jornada Basin LTER site in the northern Chihuahuan Desert, the upper limit on shrub cover is controlled by mean annual rainfall and shrub–shrub competition, as mediated by PAW variations among landforms and soil texture. Potential shrub cover generally increases as surface soil clay content increases up to 18%, possibly reflecting increases in soil fertility, then declines with further increases in clay content, perhaps related to reduced infiltration of rainfall. The simple TWI (intended as an index of rainfall redistribution) failed to explain the spatial variation in shrub cover, suggesting that more refined indices of connectivity that account for topography, soil texture, and vegetation are needed to represent the horizontal movement of water within the landscape. Inverse relationships between shrub size and density in locations with high shrub cover suggest that self-thinning occurs in most landforms, indicating the role of shrub–shrub competition in limiting maximum shrub cover in the northern Chihuahuan Desert.

A large portion of the spatial variation in shrub cover in the Jornada Basin could not, however, be explained by patterns of soil texture and associated PAW. This suggests other processes are also influencing long-term shrub establishment and mortality events. In highly variable arid and semi-arid ecosystems, underlying density dependence (i.e., competitive interactions) may impose constraints on population growth only rarely, while density-independent controls on populations (e.g., climatic events and grazing effects on shrub establishment with time lags) explain the larger fraction of landscape-scale variability in vegetation structure. In these situations, high-density landscape-scale observations, such as produced in this research, allow inference of the underlying ecological processes that

contribute to observed spatial patterns (Cale et al. 1989).

LITERATURE CITED

Archer, S. 1995. Tree-grass dynamics in a *Prosopis*-thornscrub savanna parkland: reconstructing the past and predicting the future. Ecoscience 2:83–99.

Archer, S., C. Scifres, C. R. Bassham, and R. Maggio. 1988. Autogenic succession in a subtropical savanna: conversion of grassland to thorn woodland. Ecological Monographs 58:111–127.

Archibald, S., and G. P. Hempson. 2016. Competing consumers: contrasting the patterns and impacts of fire and mammalian herbivory in Africa. Philosophical Transactions of the Royal Society B, Biological Sciences. https://doi.org/10.1098/rstb.2015.0309

Asner, G. P., S. Archer, R. F. Hughes, R. J. Ansley, and C. A. Wessman. 2003. Net changes in regional woody vegetation cover and carbon storage in Texas Drylands, 1937-1999. Global Change Biology 9:316–335.

Axelsson, C. R., and N. P. Hanan. 2017. Patterns in woody vegetation structure across African savannas. Biogeosciences 14:3239–3252.

Axelsson, C. R., and N. P. Hanan. 2018. Rates of woody encroachment in African savannas reflect water constraints and fire disturbance. Journal of Biogeography 45:1209–1218.

Basu, S., et al. 2015. A semiautomated probabilistic framework for tree-cover delineation from 1-m NAIP imagery using a high-performance computing architecture. IEEE Transactions on Geoscience and Remote Sensing 53:5690–5708.

Bestelmeyer, B. T., D. P. Goolsby, and S. R. Archer. 2011. Spatial perspectives in state-and-transition models: A missing link to land management? Journal of Applied Ecology 48:746–757.

Bestelmeyer, B. T., D. P. C. Peters, S. R. Archer, D. M. Browning, G. S. Okin, R. L. Schooley, and N. P. Webb. 2018. The grassland-shrubland regime shift in the southwestern United States: misconceptions and their implications for management. BioScience 68:678–690.

Bestelmeyer, B. T., J. P. Ward, and K. M. Havstad. 2006. Soil-geomorphic heterogeneity governs patchy vegetation dynamics at an arid ecotone. Ecology 87:963–973.

Beven, K. J., and M. J. Kirkby. 1979. A physically based, variable contributing area model of basin hydrology. Hydrological Sciences Journal 24:43–69.

Browning, D. M., S. R. Archer, G. P. Asner, M. P. McClaran, and C. A. Wessman. 2008. Woody plants in grasslands: post-encroachment stand dynamics. Ecological Applications 18:928–944.

Browning, D. M., T. M. Crimmins, D. K. James, S. Spiegal, M. R. Levi, J. P. Anderson, and D. P. C. Peters. 2018. Synchronous species responses identify phenological guilds: implications for management. Ecosphere 9:e02395.

Browning, D. M., M. C. Duniway, A. S. Laliberte, and A. Rango. 2012. Hierarchical analysis of vegetation dynamics over 71 years: soil-rainfall interactions in a Chihuahuan Desert ecosystem. Ecological Applications 22:909–926.

Browning, D. M., J. W. Karl, D. Morin, A. D. Richardson, and C. E. Tweedie. 2017. Phenocams bridge the gap between field and satellite observations in an arid grassland ecosystem. Remote Sensing 9:1071.

Buffington, L. C., and C. H. Herbel. 1965. Vegetational changes on a semidesert grassland range from 1858 to 1963. Ecological Monographs 35:139–164.

Buxbaum, C. A. Z., and K. Vanderbilt. 2007. Soil heterogeneity and the distribution of desert and steppe plant species across a desert-grassland ecotone. Journal of Arid Environments 69:617–632.

Cale, W. G., G. M. Henebry, and J. A. Yeakley. 1989. Inferring process from pattern in natural communities. BioScience 39:600–605.

Chapin, F. S. III, P. A. Matson, and P. M. Vitousek. 2011. Principles of terrestrial ecosystem ecology. Second edition. Springer, New York, New York, USA.

Choi, S., et al. 2016. Application of the metabolic scaling theory and water-energy balance equation to model large-scale patterns of maximum forest canopy height. Global Ecology and Biogeography 25:1428–1442.

Clapp, R. B., and G. M. Hornberger. 1978. Empirical equations for some soil hydraulic properties. Water Resources Research 14:601–604.

Duniway, M. C., M. D. Petrie, D. P. C. Peters, J. P. Anderson, K. Crossland, and J. E. Herrick. 2018. Soil water dynamics at 15 locations distributed across a desert landscape: insights from a 27-yr dataset. Ecosphere 9:e02335.

Eldridge, D. J., M. A. Bowker, F. T. Maestre, E. Roger, J. F. Reynolds, and W. G. Whitford. 2011. Impacts of shrub encroachment on ecosystem structure and functioning: towards a global synthesis. Ecology Letters 14:709–722.

Enquist, B. J., J. H. Brown, and G. B. West. 1998. Allometric scaling of plant energetics and population density. Nature 395:163–165.

ESRI. 2016. ArcGIS desktop, release 10.5.1. Environmental Systems Research Institute, Redlands, California, USA.

Fensham, R. J., R. J. Fairfax, and S. R. Archer. 2005. Rainfall, land use and woody vegetation cover change in semi-arid Australian savanna. Journal of Ecology 93:596–606.

Gibbens, R. P., R. P. McNeely, K. M. Havstad, R. F. Beck, and B. Nolen. 2005. Vegetation changes in the Jornada Basin from 1858 to 1998. Journal of Arid Environments 61:651–668.

Good, S. P., and K. K. Caylor. 2011. Climatological determinants of woody cover in Africa. Proceedings of the National Academy of Sciences of the United States of America 108:4902–4907.

Goslee, S. C., K. M. Havstad, D. P. C. Peters, A. Rango, and W. H. Schlesinger. 2003. High-resolution images reveal rate and pattern of shrub encroachment over six decades in New Mexico, U.S.A. Journal of Arid Environments 54:755–767.

Hacke, U. G., J. S. Sperry, J. K. Wheeler, and L. Castro. 2006. Scaling of angiosperm xylem structure with safety and efficiency. Tree Physiology 26:689–701.

Helsel, D. R., and R. M. Hirsch. 2002. Statistical methods in water resources techniques of water resources investigations, Book 4, chapter A3. U.S. Geological Survey. https://pubs.usgs.gov/twri/twri4a3/html/toc.html

Hengl, T., et al. 2017. SoilGrids250 m: global gridded soil information based on machine learning. PLoS ONE 12:e0169748.

Herbel, C. H., F. N. Ares, and R. A. Wright. 1972. Drought effects on a semidesert grassland range. Ecology 53:1084–1093.

Herrick, J. E., J. W. Van Zee, K. M. Havstad, L. M. Burkett, and W. G. Whitford. 2005. Monitoring manual for grassland, shrubland, and savanna ecosystems. USDA-ARS Jornada Experimental Range, Las Cruces, New Mexico, USA.

Huang, C., S. R. Archer, M. P. McClaran, and S. E. Marsh. 2018. Shrub encroachment into grasslands: End of an era? PeerJ 6:e5474.

Huang, C., S. E. Marsh, M. P. McClaran, and S. R. Archer. 2007. Post-fire stand structure in a semi-arid savanna: cross-scale challenges estimating biomass. Ecological Applications 17:1899–1910.

Kempes, C. P., G. B. West, K. Crowell, and M. Girvan. 2011. Predicting maximum tree heights and other traits from allometric scaling and resource limitations. PLoS ONE 6:e20551.

Koenker, R., P. Ng, and S. Portnoy. 1994. Quantile smoothing splines. Biometrika 81:673–680.

Laliberte, A. S., A. Rango, K. M. Havstad, J. F. Paris, R. F. Beck, R. McNeely, and A. L. Gonzalez. 2004. Object-oriented image analysis for mapping shrub encroachment from 1937 to 2003 in southern New Mexico. Remote Sensing of Environment 93:198–210.

Lehmann, C. E. R., et al. 2014. Savanna vegetation-fire-climate relationships differ among continents. Science 343:548–552.

Ludwig, J. A., R. W. Eager, G. N. Bastin, V. H. Chewings, and A. C. Liedloff. 2002. A leakiness index for assessing landscape function using remote sensing. Landscape Ecology 17:157–172.

Ludwig, J. A., B. P. Wilcox, D. D. Breshears, D. J. Tongway, and A. C. Imeson. 2005. Vegetation patches and runoff-erosion as interacting ecohydrological processes in semiarid landscapes. Ecology 86:288–297.

McAuliffe, J. R. 1994. Landscape evolution, soil formation, and ecological patterns and processes in Sonoran Desert bajadas. Ecological Monographs 64:111–148.

McGlynn, I. O., and G. S. Okin. 2006. Characterization of shrub distribution using high spatial resolution remote sensing: ecosystem implications for a former Chihuahuan Desert grassland. Remote Sensing of Environment 101:554–566.

Monger, H. C., and B. T. Bestelmeyer. 2006. The soil-geomorphic template and biotic change in arid and semi-arid ecosystems. Journal of Arid Environments 65:207–218.

Monger, H. C., G. H. Mack, B. A. Nolen, and L. H. Gile. 2006. Regional setting of the Jornada basin. Pages 15–43 in K. M. Havstad, L. F. Huenneke, and W. H. Schlesinger, editors. Structure and function of a Chihuahuan Desert ecosystem. Oxford University Press, New York, New York, USA.

Monger, H. C., O. E. Sala, M. C. Duniway, H. Goldfus, I. A. Meir, R. M. Poch, H. L. Throop, and E. R. Vivoni. 2015. Legacy effects in linked ecological-soil-geomorphic systems of drylands. Frontiers in Ecology and the Environment 13:13–19.

Noy-Meir, I. 1973. Desert ecosystems: environment and producers. Annual Review of Ecology and Systematics 4:25–51.

Parker, K. C. 1995. Effects of complex geomorphic history on soil and vegetation patterns on arid alluvial fans. Journal of Arid Environments 30:19–39.

Peters, D. P. C., B. T. Bestelmeyer, J. E. Herrick, E. L. Fredrickson, H. C. Monger, and K. M. Havstad. 2006. Disentangling complex landscapes: new insights into arid and semiarid system dynamics. BioScience 56:491–501.

Peters, D. P. C., J. E. Herrick, H. C. Monger, and H. Huang. 2010. Soil-vegetation-climate interactions in arid landscapes: effect of the North American monsoon on grass recruitment. Journal of Arid Environments 74:618–623.

Rachal, D. M., H. C. Monger, G. S. Okin, and D. P. C. Peters. 2012. Landform influences on the resistance of grasslands to shrub encroachment, Northern Chihuahuan Desert, USA. Journal of Maps 8:507–513.

Rampi, L. P., J. F. Knight, and C. F. Lenhart. 2014. Comparison of flow direction algorithms in the application of the CTI for mapping wetlands in Minnesota. Wetlands 34:513–525.

Rango, A., J. C. Ritchie, W. P. Kustas, T. J. Schmugge, and K. M. Havstad. 1998. JORNEX: remote sensing to quantify long-term vegetation change and hydrological fluxes in an arid rangeland environment. Pages 585–590 in H. Wheater and C. Kirby, editors. Hydrology in a changing environment. John Wiley & Sons, Chichester, Sussex, UK.

Rango, A., K. A. Snyder, J. E. Herrick, K. M. Havstad, R. P. Gibbens, J. Wainwright, and T. Parsons. 2003. Historical and current hydrological research at the USDA/ARS Jornada Experimental Range in southern New Mexico. Pages 302–308 in K. G. Renard, S. A. McElroy, W. J. Gburek, E. H. Canfield, and R. L. Scott, editors. First Interagency Conference on Research in the Watersheds, Benson, Arizona, October 27-30, 2003. U.S. Department of Agriculture, Agricultural Research Service, Beltsville, Maryland, USA.

Reynolds, J. F., R. A. Virginia, P. R. Kemp, A. G. de Soyza, and D. C. Tremmel. 1999. Impact of drought on desert shrubs: effects of seasonality and degree of resource island development. Ecological Monographs 69:69–106.

Roques, K. G., T. G. O'Connor, and A. R. Watkinson. 2001. Dynamics of shrub encroachment in an African savanna: relative influences of fire, herbivory, rainfall and density dependence. Journal of Applied Ecology 38:268–280.

Ross, C. W., L. Prihodko, J. Anchang, S. Kumar, W. Ji, and N. P. Hanan. 2018. HYSOGs250 m, global gridded hydrologic soil groups for curve-number-based runoff modeling. Scientific Data 5:180091.

Ryan, M. G., and B. J. Yoder. 1997. Hydraulic limits to tree height and tree growth. BioScience 47:235–242.

Sankaran, M., J. Ratnam, and N. P. Hanan. 2004. Tree-grass coexistence in savannas revisited-insights from an examination of assumptions and mechanisms invoked in existing models. Ecology Letters 7:480–490.

Sankaran, M., et al. 2005. Determinants of woody cover in African savannas. Nature 438:846–849.

Scholes, R. J., and S. R. Archer. 1997. Tree-grass interactions in savannas. Annual Review of Ecology and Systematics 28:517–544.

Scholtz, R., S. D. Fuhlendorf, and S. R. Archer. 2018. Climate-fire interactions constrain potential woody plant cover and stature in North American Great Plains grasslands. Global Ecology and Biogeography 27:936–945.

Schooley, R. L., B. T. Bestelmeyer, and A. Campanella. 2018. Shrub encroachment, productivity pulses, and core-transient dynamics of Chihuahuan Desert rodents. Ecosphere 9:e02330.

Sea, W. B., and N. P. Hanan. 2012. Self-thinning and tree competition in savannas. Biotropica 44:189–196.

Sperry, J. S., and U. G. Hacke. 2002. Desert shrub water relations with respect to soil characteristics and plant functional type. Functional Ecology 16:367–378.

Van Auken, O. W. 2000. Shrub invasions of North American semiarid grasslands. Annual Review of Ecology and Systematics 31:197–215.

Ward, D., K. Wiegand, and S. Getzin. 2013. Walter's two-layer hypothesis revisited: back to the roots!. Oecologia 172:617–630.

Weller, D. E. 1987. A reevaluation of the -3/2 power rule of plant self-thinning. Ecological Monographs 57:23–43.

Wheeler, C. W., S. R. Archer, G. P. Asner, and C. R. McMurtry. 2007. Climatic/edaphic controls on soil carbon/nitrogen response to shrub encroachment in desert grassland. Ecological Applications 17:1911–1928.

Whitford, W. G. 1996. The importance of the biodiversity of soil biota in arid ecosystems. Biodiversity & Conservation 5:185–195.

Whitford, W. G., and B. T. Bestelmeyer. 2006. Chihuahuan desert fauna: effects on ecosystem properties and processes. Pages 247–265 *in* K. M. Havstad, L. F. Huenneke, and W. H. Schlesinger, editors. Structure and function of a Chihuahuan Desert ecosystem. Oxford University Press, New York, New York, USA.

Wu, X. B., and S. R. Archer. 2005. Scale-dependent influence of topography-based hydrologic features on patterns of woody plant encroachment in savanna landscapes. Landscape Ecology 20:733–742.

Supporting Information